27th ABCM International Congress of Mechanical Engineering
December 04-08, 2023, Florianópolis-SC, Brazil

COB-2023-1545
THE VISUALEFM.JL PACKAGE FOR WIND TUNNEL STUDIES OF PEDESTRIAN-LEVEL WIND USING SAND EROSION TECHNIQUE

Gabriel Borelli Martins
Felipe Augusto Frazão Kleine
Instituto de Pesquisas Tecnológicas do Estado de SP. Av. Prof. Almeida Prado, 532, Cid. Universitária - Butantã. São Paulo/SP
gborelli@ipt.br
fkleine@ipt.br

Abstract. *Sand erosion can be an useful technique applied in wind tunnel studies of pedestrian-level wind comfort, heat islands and contaminant dispersion in urban environments. The technique generates a large amount of images which can make analysis and decision-making difficult. Image processing can help with that, by creating clearer color maps and animations. A specific image processing workflow was included to the new VisualEFM Julia package to simplify the extraction of sand erosion patterns from wind tunnel tests. To develop the package a 1:500 scaled model of an urban area in São Paulo was tested in the Atmospheric Boundary Layer Wind Tunnel of the Institute for Technological Research (IPT). The procedure adopted was able to automatically extract the erosion patterns and proved to be very useful for wind tunnel studies involving the ventilation in urban environments.*

Keywords: *ventilation, sand erosion, wind tunnel, image processing.*

1. INTRODUCTION

The urban environment is constantly changing. New buildings and structures modify the wind flow, affecting the ventilation inside urban areas. These changes can have critical implications, particularly when considering the pollutant dispersion near congested avenues and the comfort and safety of pedestrians.

Wind tunnels are useful tools to simulate pedestrian-level wind characteristics, although near wall measurements are difficult considering the air flow complexities observed in urban canopies. Specific omnidirectional sensors can be applied to measure mean wind velocities on wind tunnel models, such as the pressure sensor proposed by Irwin (1981), hotwire anemometers and the thermistor anemometer developed by Jabardo *et al.* (2019). The allocation of such sensors on the model's surface might be challenging depending on the number of devices available and on how large the study area is.

For large flat models, the sand erosion is a qualitative technique that can be applied to identify critical regions. Usually, these regions are related to areas of low ventilation, leading to pollutant dispersion issues and heat island formation, or areas of high wind velocities, which can lead to pedestrian discomfort or even danger (specially for the elderly and the people with mobility impairments). After identifying these critical regions, complementary studies can be carried out, including those aimed to obtain reliable mean wind velocities using specific sensors as those aforementioned.

During a sand erosion test several digital pictures are taken from the erosion patterns formed. The idea behind the VisualEFM package is to apply image processing techniques to produce color maps and animations from the patterns, which can help with interpretation and decision-making.

2. THE SAND EROSION TECHNIQUE FOR WIND TUNNEL STUDIES

The sand erosion technique is described in detail by Borges and Saraiva (1979). Basically it consists in spreading a thin layer of sand with small and controlled granularity on the model's surface, increasing the wind tunnel speed step by step, taking pictures and analyzing the erosion patterns formed. The tests are repeated for different wind headings.

For each step sand erosion is allowed to last long enough to try to reach contours stability. A previous calibration is usually done in order to estimate the friction velocity threshold, for which the grains of sand are carried by the wind. A digital camera is used to take pictures of the stabilized erosion patterns. Finally, a amplification factor C_V, defined as the ratio between the local and the reference wind velocity, can be found (Blocken *et al.*, 2016).

If the layer of sand is kept thin, with loose grains, then the Reynolds number will be smaller than 5 and the grains of sand will be located inside the viscous sub-layer, which means sand saltation will not depend on the velocity profile nor on the boundary layer thickness (Jabardo *et al.*, 2005). Assuming Reynolds number independence, which is a reasonable assumption for an urban area full of buildings with sharp edges (Jabardo *et al.*, 2005), then

$$\frac{v_\tau}{v_\tau^0} \approx \frac{V_{ref}}{V_{pic}} = C_V \tag{1}$$

where v_τ is the local friction velocity, v_τ^0 is the reference friction velocity (from calibration), V_{pic} is the wind tunnel velocity at a reference height when the picture of a erosion pattern was taken and V_{ref} is the velocity at the same reference height obtained during the calibration process when the grains of sand start to be carried by the wind.

This technique has the advantage to cover large areas with the same wind tunnel test, pointing out possible problematic regions. These regions can be the ones of low wind velocities or of high wind velocities, as mentioned before. On the other hand, this technique is restricted to flat surfaces, can present low accuracy in areas of high turbulence intensity and is influenced by the size, the shape and the arrangement of the sand particles (Blocken *et al.*, 2016).

3. METHODOLOGY

A Julia package, called VisualEFM (Martins, 2020) was developed in order to deal with the several digital images taken during the sand erosion tests. This package helps to create animations and color maps of the erosion observed during the tests by the use of classical image processing techniques, already implemented in other Julia packages, applied in a specific sequence. The novelty of the VisualEFM lies on the workflow and on the resulting plots for the application discussed in this paper.

A 1:500 scaled model of an urban area in the east region of São Paulo was manufactured to test the workflow proposed on this paper. The model was manufactured in MDF and painted black in order to increase the contrast between the background and the grains of sand. The tests were done in IPT's Atmospheric Boundary Layer Wind Tunnel, located in São Paulo, Brazil.

3.1 The boundary layer wind tunnel

A side view draft of the IPT's Atmospheric Boundary Layer Wind Tunnel, used for the tests that helped on the VisualEFM development, is shown in Fig. 1. It is a 41 m long open-circuit wind tunnel constructed for wind engineering studies. Its test section is 3 m wide and 2 m high.

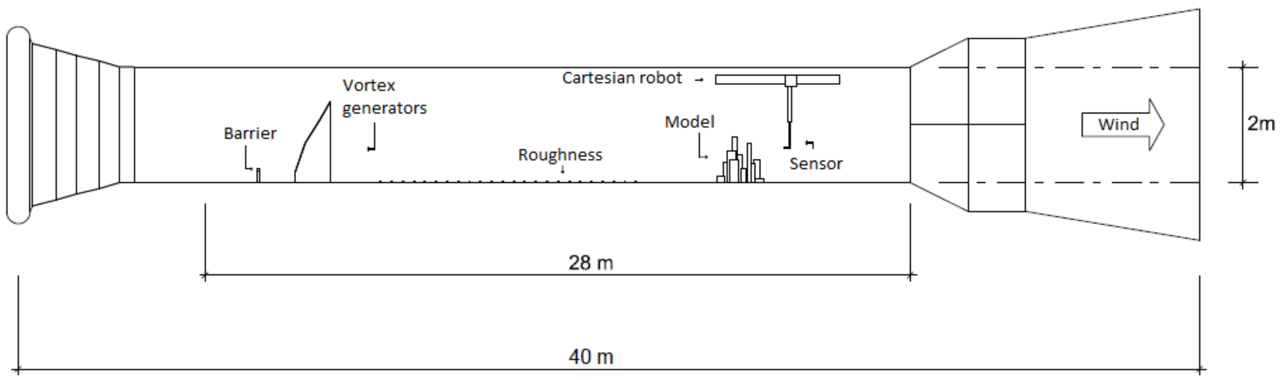

Figure 1. Side view draft of IPT's Atmospheric Boundary Layer Wind Tunnel.

3.2 Image acquisition

For the image acquisition it is important to notice that the camera must be firmly attached at the same position for the whole test. The pattern identification is based on the subtraction of consecutive images and thus if the camera is moved, no valid pattern will be identified. Small vibrations are not a problem, providing they are limited and the camera position is not changed after the wind tunnel is turned off. The contrast between the grains of sand and the model's background should be as high as possible to help with the identification of the erosion patterns, hence the MDF model was painted black as already mentioned. Also, the illumination setup must be kept fixed during the process. It might be interesting to perform a camera calibration to correct some of the distortion if dimensional measurements are required. This was not a concern for the tests proposed in this paper.

The main procedure consists in taking a picture at the beginning of the test, when the wind tunnel is not running and there are no erosion patterns. Then the wind tunnel speed is increased step by step and one image for each step is captured. The elapsed time for each step is an important parameter. Regions with high turbulence intensities may present larger erosion patterns than it would be if the mean friction velocities were applied, resulting in higher uncertainties. Elapsed times between 1 and 2 minutes were reported by Blocken *et al.* (2016) to present good repeatability of the erosion patterns.

3.3 The VisualEFM image processing workflow

The image processing techniques applied for the segmentation of the erosion patterns, as well as the sequence, are similar to those explained by Martins *et al.* (2018). All these techniques are described in great detail by Gonzalez and Woods (2007). It is important to mention that no color information is necessary for the method proposed, therefore only grayscale images are used.

The first step is to reduce the high spatial frequency information with a low-pass filter (LPF). The LPF will remove undesirable high frequency noise. The algorithm proposed applies a Gaussian filter, hence erosion edges do not get too blurred. It is important to apply the same filter type and size for all the images obtained during the tests in order to preserve the perimeters of erosion patterns.

To extract a erosion pattern, two images in sequence are required. The grayscale images are subtracted and then the result is converted to binary. Any desired algorithm can be used to determine the threshold value, but the Otsu's algorithm was applied for the case studied. This is a good choice to recognize two regions in the grayscale histogram, as it is observed in Fig. 2. For a non homogeneous illumination scenario, an adaptive method might be a better choice.

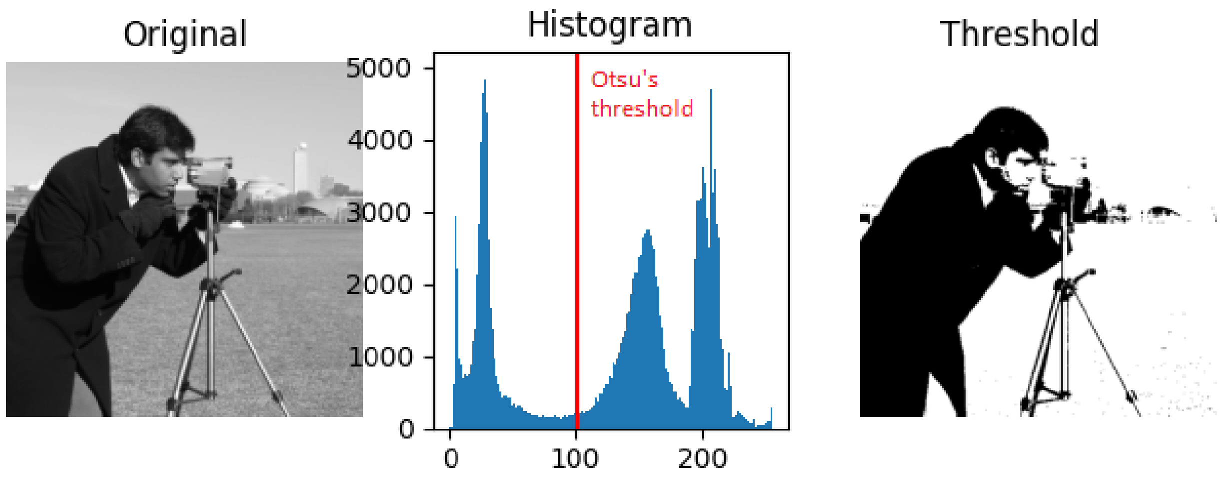

Figure 2. Image thresholding using Otsu's algorithm (Van der Walt *et al.*, 2014).

Finally, small undesired spaces between grains of sand can be removed with morphological closing. The closing operation $A \cdot B$ consists in two morphological operations applied in sequence.

$$A \cdot B = (A \oplus B) \ominus B \tag{2}$$

The first morphological operation is dilatation, which seeks to remove the small and undesired empty spaces between the grains of sand. Presented by the $\oplus$ operator, the dilatation of A by the element B results in a z set of displacements which the translation of $\hat{B}$ (symmetric of B) by z is equivalent to a subset of A (Gonzalez and Woods, 2007).

$$A \oplus B = \{z | (\hat{B})_z \cap A \neq \varnothing\} \tag{3}$$

However, this operation also increases the erosion pattern perimeter. That is why an opposite morphological operation, the erosion, is necessary. Presented by the $\ominus$ operator, the erosion of A by the element B results in a z set of displacements which the translation of B by z has always a element of A (Gonzalez and Woods, 2007).

$$A \ominus B = \{z | (B)_z \subseteq A\} \tag{4}$$

The closing process tends to smooth the object contour, to merge the narrow breaks, to eliminate small holes and to fill the gaps in the contour of the images. The closing operation given in Eq. 2 is illustrated in Fig. 3. It is important to apply the same kernel for both dilatation and erosion, hence the main pattern size is neither increased nor reduced.

The resulting image is labeled using the C_V values obtained during the tests. A workflow of the whole process is given in Fig. 4, while Fig. 5 shows the result for each step of the workflow.

The image processing sequence proposed was implemented in the Julia package VisualEFM (Martins, 2020). All commands and functionalities are fully explained in the package documentation.

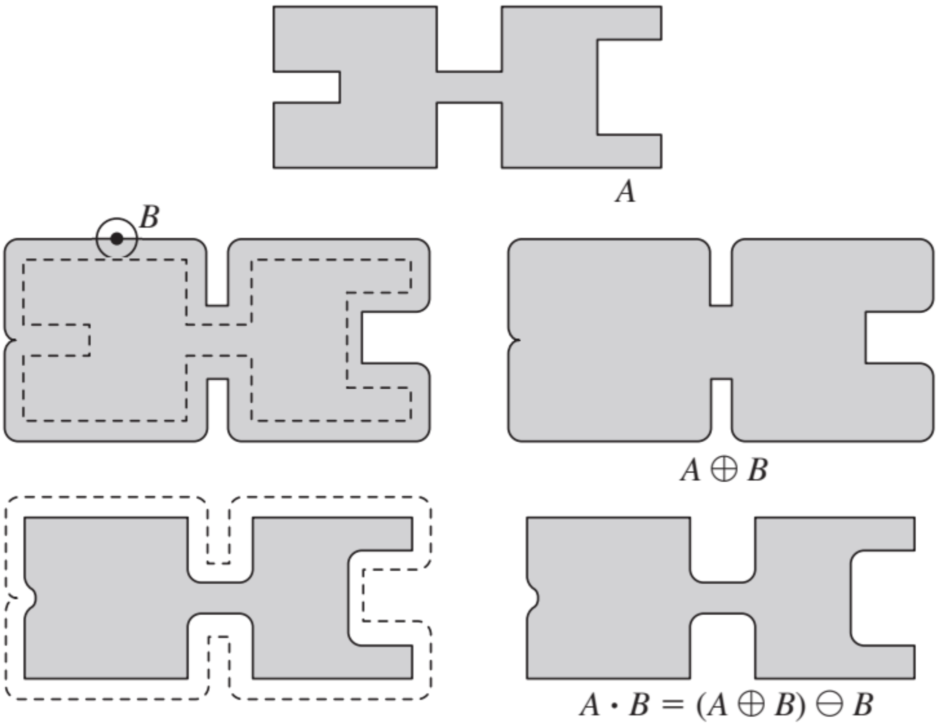

Figure 3. Illustration of the closing operation of image A by the kernel B (adapted from Gonzalez and Woods (2007)).

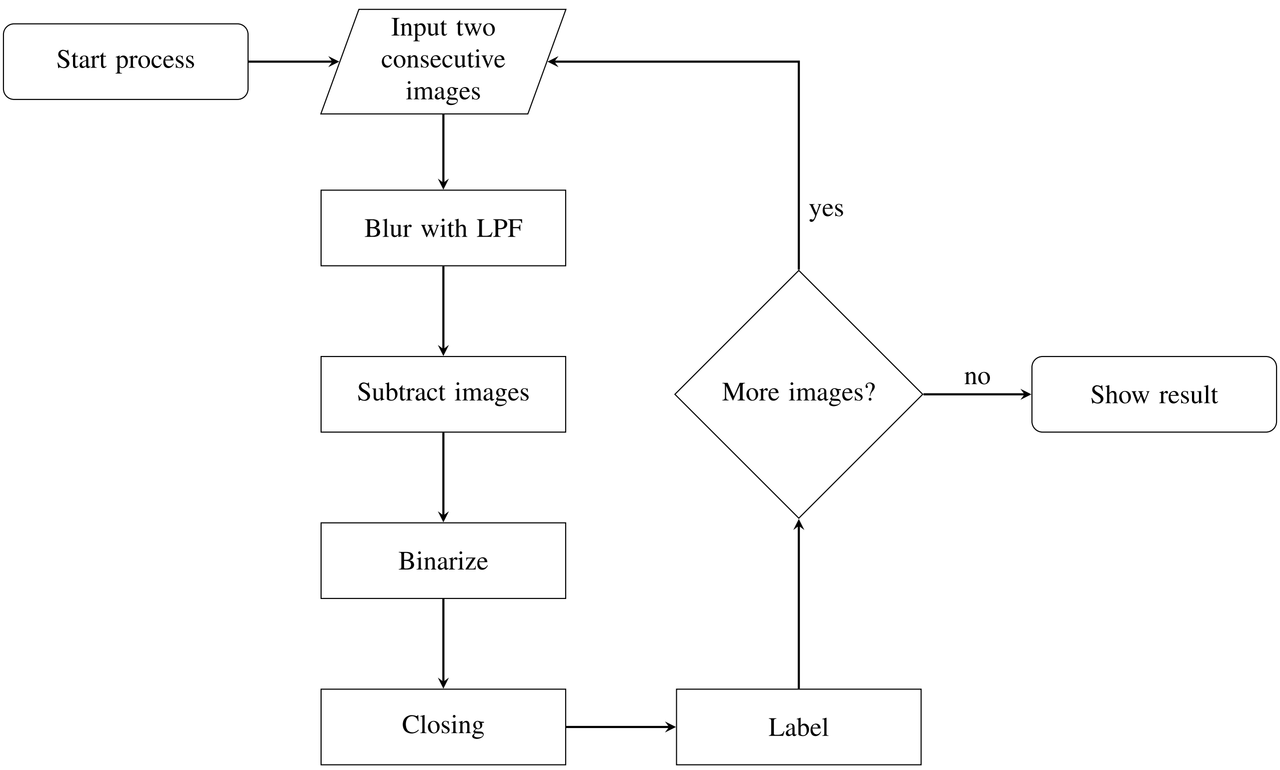

Figure 4. Sand erosion image processing workflow.

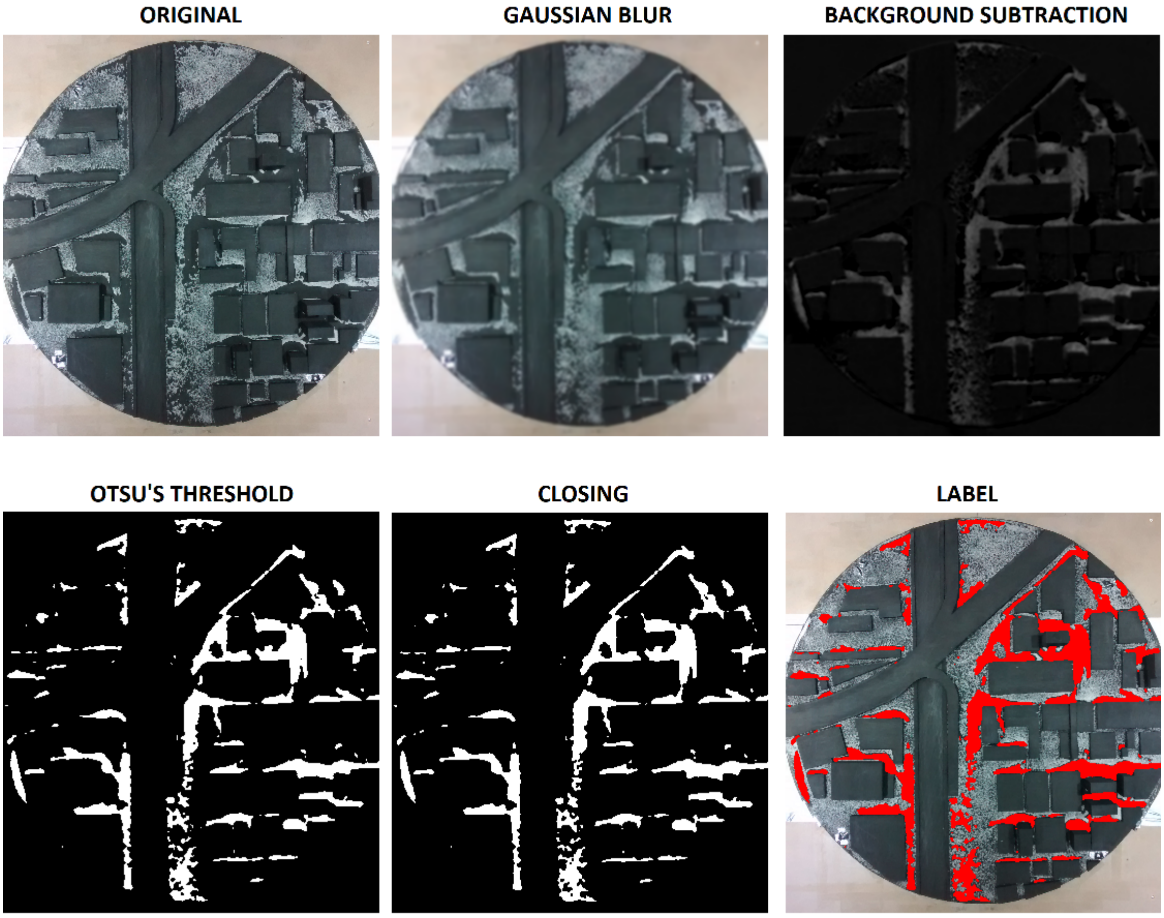

Figure 5. Steps of the VisualEFM workflow.

3.4 Testing procedure

The wind velocities were measured at a height of 48 mm in the wind tunnel, which is equivalent to a height of 24 m in real case considering the 1:500 length scale. A previous calibration on a flat surface alone determined the velocity of 8.2 m/s for which the friction velocity on the surface reaches the threshold value and sand saltation occurs. The model was installed on the wind tunnel turntable and a thin layer of sand was poured on the flat region as shown in Fig. 6.

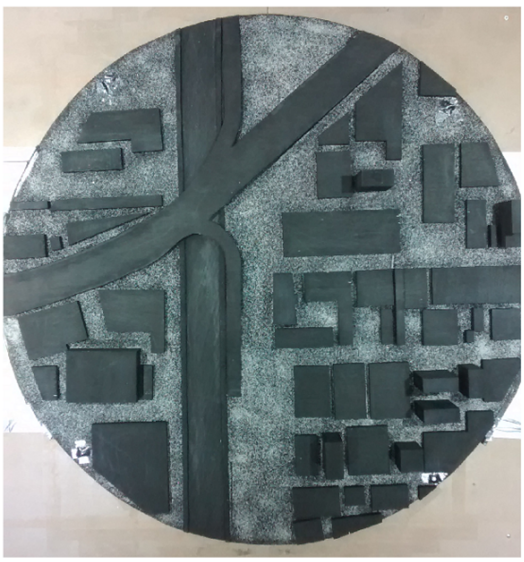

Figure 6. Image of the initial setup without any erosion patterns.

The tests were done for one wind heading (east) and 10 different velocities, given in Tab. 1. For each velocity a different erosion pattern was produced and a picture was taken. All the erosion patterns were then segmented and labeled using the image processing techniques described in Section 3.3

Table 1. Wind tunnel test velocities at a reference height.

$\mathbf{V_{pic}}$ (m/s)	$\mathbf{C_V}$
4.4	1.86
5.2	1.58
6.0	1.37
6.9	1.19
7.7	1.06
8.4	0.98
9.0	0.91
9.7	0.85
11.1	0.74
12.7	0.65

4. RESULTS

For each velocity presented in Tab. 1 an erosion pattern was extracted using the tools provided in the VisualEFM package. An example is shown in the Fig. 7. The Fig. 7a shows the picture obtained during the tests for V_{pic} = 6.0 m/s while the Fig. 7b presents the segmented patterns (in red) produced using the initial picture presented in Fig. 6 for background subtraction.

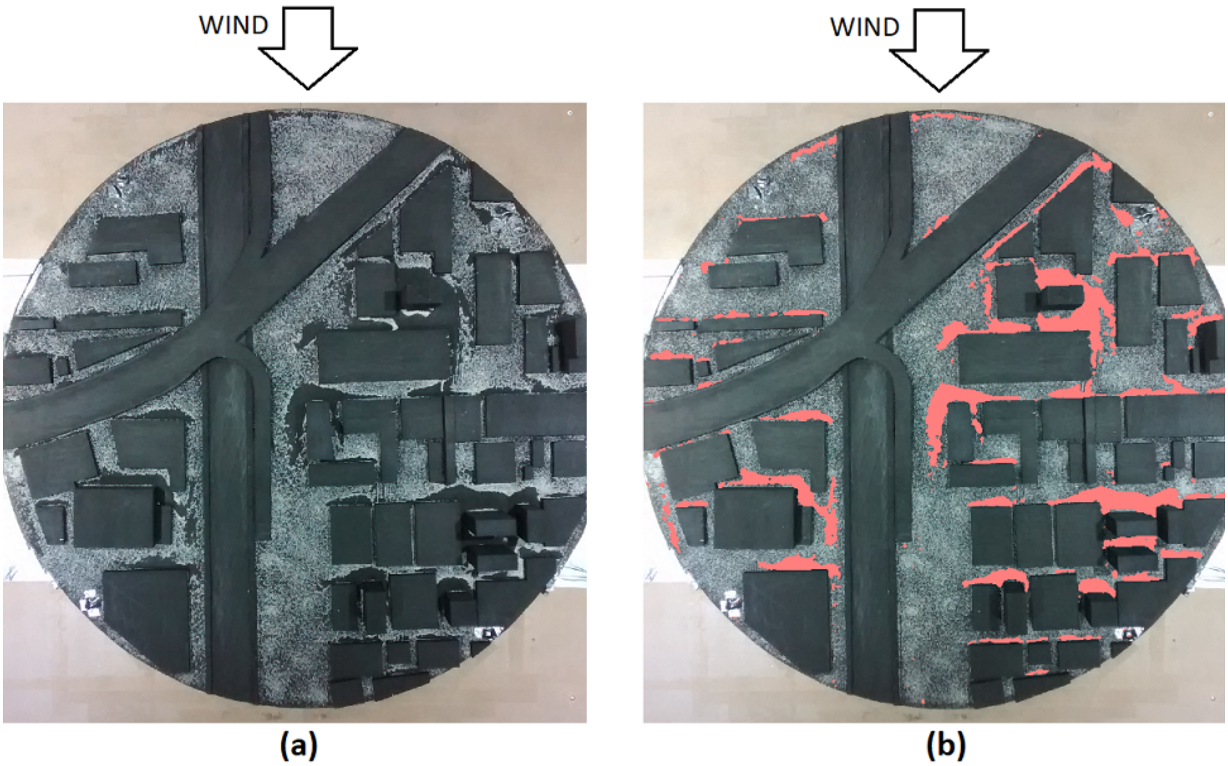

Figure 7. Erosion picture for V_{pic} equals to 6.0 m/s (a) and the segmented erosion pattern in red (b).

When segmentation is done for all the pictures taken during the wind tunnel tests, one can visualize the whole erosion process through a color map, as shown in Fig. 8. Figure 8 shows the near wall regions with higher velocities, in yellow, orange and red. As expected, regions near building edges and near the frontal façades presented the higher C_V values (red), indicating they should be further investigated when dealing with pedestrian-level wind comfort studies. A vegetation covering policy can be addressed based on the results presented by this map, for example. For the wind heading considered (east), the mean C_V value near the avenue located in the center of the model is a little bit higher than one, indicating better ventilation than those observed on some areas between buildings, where the C_V is smaller than one.

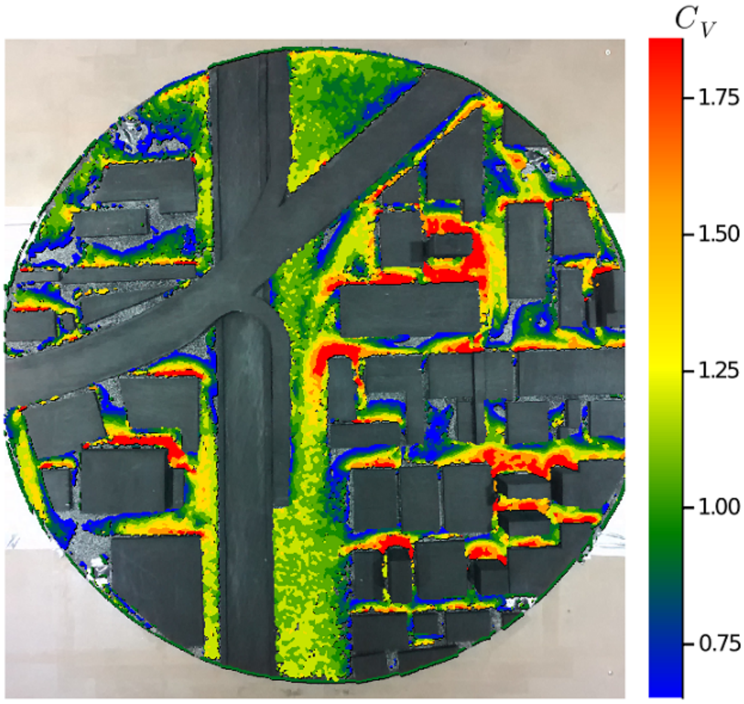

Figure 8. Erosion map obtained after a full run on specific wind heading.

Depending on the study to be done, it might be necessary to put in evidence particular regions of the model. This can be easily achieved by the use of masks. A mask is a binary matrix and can reproduce complex geometry, such the one on the left of Fig. 9. The result is the same map obtained on Fig. 8, but with the undesired regions suppressed.

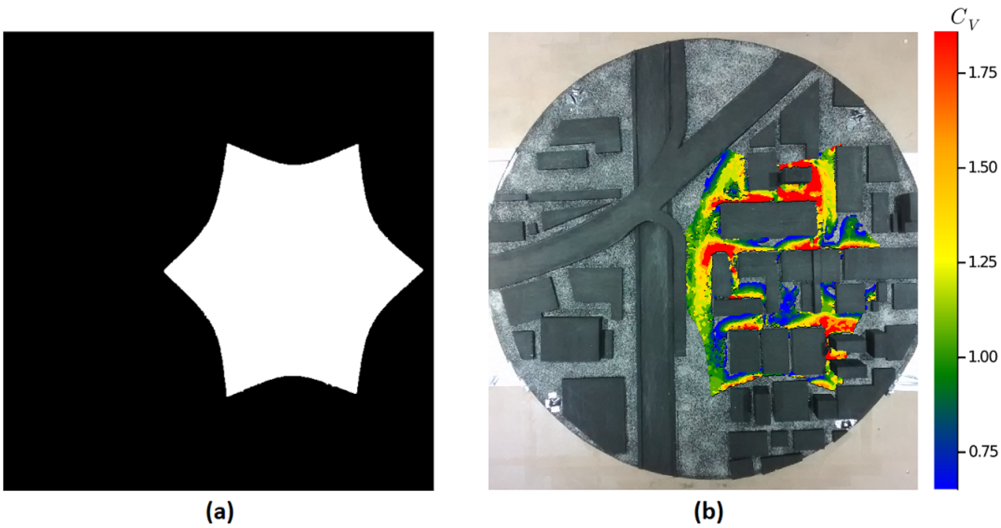

Figure 9. Mask (a) applied to highlight a region of the erosion map (b).

5. CONCLUSION

Although the sand erosion technique can be very inaccurate for near surface velocity estimation, especially in the cases where high turbulence is presented, it is still an useful technique to be applied in wind tunnel studies of large urban areas. High velocity and low velocity regions can be easily identified and then be measured with greater accuracy by other sensors, such as the Irwin's pressure sensor, the Jabardo's thermistor sensor or hotwire anemometers.

Usually several wind headings and repetitions are required, resulting in a large number of images which might be difficult to analyze. Moreover, showing a large number of pictures to the policymakers is not feasible. By correctly identifying the erosion patterns and creating color maps or animations, the VisualEFM package is a helpful tool for wind tunnel technicians.

6. ACKNOWLEDGEMENTS

We thank the IPT's wind tunnel technicians for helping with the tests.

7. REFERENCES

Blocken, B., Stathopoulos, T. and Van Beeck, J., 2016. "Pedestrian-level wind conditions around buildings: Review of wind-tunnel and cfd techniques and their accuracy for wind comfort assessment". *Building and Environment*, Vol. 100, pp. 50–81.

Borges, A.R.J. and Saraiva, J.A.G., 1979. "An erosion technique for assessing ground level winds". In *Proceedings of the Fifth International Conference On Wind Engineering*. Fort Collins, Colorado, USA, Vol. 1, pp. 235–242.

Gonzalez, R.C. and Woods, R.E., 2007. *Digital Image Processing*. Pearson.

Irwin, H.P.A.H., 1981. "A simple omnidirectional snsor for wind-tunnel studies of pedestrian-level winds". *Journal of Wind Engineering and Industrial Aerodynamics*, Vol. 7, No. 3, pp. 219–239.

Jabardo, P.J.S., Alves, L., Martins, G.B. and Nader, G., 2019. "Low cost anemometers for wind tunnel and ventilation applications". *Revista IPT: Tecnologia e Inovação*, Vol. 2, No. 10.

Jabardo, P.J.S., Prata, A.R., Marciotto, E.R. and Nader, G., 2005. "Influence of integral length scales on sand erosion techniques". In *Proceedings of the COBEM 2002: 18th International Congress of Mechanical Engineering*. ABCM - Brazilian Society of Mechanical Sciences and Engineering, Ouro Preto, MG, Brazil.

Martins, G.B., 2020. "Visualefm.jl (julia package)". Github repository. https://github.com/tunelipt/VisualEFM.jl.

Martins, G.B., Costa, A.B., Jabardo, P.J.S. and Nader, G., 2018. "Near wall measurements for pedestrian comfort studies in wind tunnels (in portuguese)". *Revista IPT: Tecnologia e Inovação*, Vol. 2.

Van der Walt, S., Schönberger, J.L., Nunez-Iglesias, J., Boulogne, F., Warner, J.D., Yager, N., Gouillart, E. and Yu, T., 2014. "scikit-image: image processing in python". *PeerJ*, Vol. 2, p. e453.

8. RESPONSIBILITY NOTICE

The authors are solely responsible for the printed material included in this paper.